Applied Catalysis A: General 507 (2015) 26–33

Contents lists available at ScienceDirect

Applied Catalysis A: General

journal homepage: www.elsevier.com/locate/apcata

Room temperature hydrogenation of furfuryl alcohol by Pd/titanate nanotube

Qingqing Yuan, Feiyang Ye, Teng Xue, Yejun Guan*

Shanghai Key Laboratory of Green Chemistry and Chemical Processes, School of Chemistry and Molecular Engineering, East China Normal University, North Zhongshan Road 3663, Shanghai 200062, China

ARTICLE INFO

Article history:
Received 11 June 2015
Received in revised form 4 September 2015
Accepted 23 September 2015
Available online 28 September 2015

Keywords:
Palladium
Furfuryl alcohol
Hydrogenation
Tetrahydrofurfuryl alcohol
Titanate nanotube

ABSTRACT

The liquid phase hydrogenation of furfuryl alcohol to tetrahydrofurfuryl alcohol at room temperature under 1 atm hydrogen was succeeded on a TiO_2 nanotube (TNT) supported palladium catalyst. The palladium nanoparticles in size of 2–8 nm were loaded by the deposition-reduction method with $NaBH_4$ as reducing reagent. The Pd/TNT catalyst showed high dispersion as revealed by CO chemisorption and improved catalytic performance in terms of both furfuryl alcohol conversion and tetrahydrofurfuryl alcohol selectivity, probably attributed to the unique electronic interaction between Pd metals and TNT surface containing sodium cations. Among the catalysts investigated, 5.8 wt.% Pd/TNT showed the best performance, with 98% conversion and 98% selectivity to tetrahydrofurfuryl alcohol in ethanol.

1. Introduction

Synthesis of tetrahydrofurfuryl alcohol (THFA) from either furfural (FAL) or furfuryl alcohol (FA) is of great industrial interests because THFA is an environmentally benign and biodegradable furanic chemical with low toxicity. It has been broadly used as both intermediate and green solvent in agricultural and industrial applications [1,2]. Recently, THFA has also been proposed to be a promising substrate for the preparation of diols [3,4]. Conventionally THFA is produced by a two-step catalytic hydrogenation of FAL via FA as intermediate over Cu–Cr, Ni or noble metal catalysts [5,6]. The second step of FA hydrogenation commonly involves high temperature (>100 °C) and high H_2 pressure (3–6 MPa) [7–15]. Gowda et al. [7] reported a homogeneous Ru(II) bis(diimine) catalyst for hydrogenating FA into THFA under 130 °C, 5 MPa H_2, with 99% selectivity. The difficulties encountered in separation and loss of metal centers strongly limit the practical application of homogeneous catalysts [16]. Adkins and Connor [8] in 1931, for the first time reported the hydrogenation of FA using a heterogeneous Cu–Cr catalyst. The reaction was carried out in liquid phase for 11.5 h at 175 °C and 10–15 MPa hydrogen with THFA yield being less than 10%. A higher THFA selectivity of 48% was achieved over a Raney nickel catalyst under modest temperature [9]. Supported nickel catalysts have been reported to be selective for the synthesis of THFA under very harsh reaction conditions such as 180 °C, 3–4 MPa H_2 and 3.5 h [10–13]. Zhang et al. [14] emphasized the hydrogenation of FA over a series of MnO_x supported Ru, Pd, Pt and Rh catalysts at 120 °C, 3–6 MPa for 4 h in an aqueous phase and the Ru/MnO_x showed the best catalytic performance with 79% yield to THFA. Under harsher conditions (220 °C, 3.5 MPa H_2) the Pd/C catalyst showed full conversion of FA to THFA in isopropanol solvent after 5 h [15]. A main drawback of hydrogenation at high temperature is the possible formation of various by-products, such as 2-methylfuran (MF), tetrahydrofuran, 1, 2-pentanediol and 1, 5-pentanediol [8,9,11–15]. Recently, Khan et al. [17] reported a mild hydrogenation process which described the FA hydrogenation on a hectorite-supported Ru nanoparticles in methanolic solution at 40 °C under a hydrogen pressure of 20 bar and the THFA yield reached 99%. Therefore, selective synthesis of THFA under mild reaction condition is an attractive alternative method to the conventional ones.

In this study we report the successful hydrogenation of FA under ambient conditions catalyzed by a Pd-supported sodium-titanate nanotube catalyst, which shows unprecedented activity and selectivity to THFA at room temperature and 1 bar H_2. The sodium cations in the titanate are thought to play a crucial role in stabilizing well-dispersed Pd metal particles as well as inhibiting MF formation.

* Corresponding author. Fax: +86 2132530334.
E-mail address: yjguan@chem.ecnu.edu.cn (Y. Guan).

http://dx.doi.org/10.1016/j.apcata.2015.09.034
0926-860X/

2. Experimental

2.1. Preparation of catalysts

Titanate nanotubes (TNT) were prepared according to the reference [18]. Typically, commercial anatase-type TiO_2 (2 g) was added to 100 mL of NaOH aqueous solution (10 M). After being stirred for 10 min, the mixture was transferred into a Teflon-lined (120 mL) stainless steel autoclave and statically heated in an oven at 130 °C for 72 h. The white product was filtered and washed with large amount of deionized water until the pH was 7. The final products were subsequently dried at 110 °C overnight, calcined at various temperatures (400, 600 and 800 °C) for 3 h and labeled as TNT-T (400, 600 and 800, respectively).

For comparison, we also prepared the proton-exchanged TNT with 0.1 M HCl solution to investigate the acid-base properties of TNT samples. After that, the mixture was filtered, washed thoroughly with deionized water and dried at 110 °C and labeled as TNT-H.

Pd supported on commercial anatase-type TiO_2 or TNTs were prepared using a deposition-reduction method. The support (0.5 g) was dispersed in H_2O (60 mL) with stirring. A specified amount of H_2PdCl_4 aqueous solution (21.512 g_{Pd}/L) was added to the mixture and stirred for 3 h. The final pH value of the suspension was adjusted to 10 by adding NaOH solution (1 M). Then, $NaBH_4$ aqueous solution ($NaBH_4$/Pd = 10, molar ratio) was added into the suspension and the mixture was stirred for another 30 min allowing for the full reduction of Pd^{2+} species. Thus obtained catalyst was dried at 110 °C overnight.

2.2. Catalyst characterization

Nitrogen adsorption–desorption isotherms at −196 °C were obtained on a BELSORP-Max equipment. Prior to the measurement, the samples were first degassed at 150 °C under vacuum for 6 h. Specific surface areas (SSA) were calculated according to the Brunauer–Emmett–Teller (BET) method using five relative pressure points in the interval of 0.05–0.30. The pore size distribution was obtained by the BJH model applied to the adsorption isotherm.

Pulse CO chemisorption was performed on a Micromeritics AutoChem 2910 to determine the metal dispersion of the reduced catalysts. Prior to measurement, the catalyst was reduced in a flow of 80 mL/min 10 vol.% H_2 in Ar at 80 °C for 2 h and then cooled to 30 °C by flushing He for 2 h. Afterwards, CO gas pluses (5 vol.% in He) were introduced in a flow of 110 mL/min. The gas phase CO concentration was followed by thermal conductivity detector (TCD).

The Pd loading was quantified by inductively coupled plasma (ICP) on a Thermo IRIS Intrepid II XSP atomic emission spectrometer. About 5 mg catalysts were digested using 10 mL of aqua regia. The obtained solutions were diluted with deionized water before test.

The power X-ray diffraction (XRD) patterns were collected on a Rigaku Ultima IV X-ray diffractometer using Cu Kα radiation (λ = 1.5405 Å) operated at 35 kV and 25 mA. Scanning electron microscopy (SEM) was performed on a Hitachi S-4800 microscope. Transmission electron microscopy (TEM) images were taken on a FEI Tecnai G^2 F30 microscope operating at 300 kV. The average Pd particle size was calculated by $d_{TEM} = (\Sigma n_i d_i^3)/(\Sigma n_i d_i^2)$ by measuring at least 100 particles. Temperature-programmed desorption of NH_3 (NH_3-TPD) testing was performed using a TP-5080 chemisorption instrument (Xianquan Co., Ltd., Tianjin, China) with a thermal conductivity detector (TCD). After pretreatment at 400 °C under flowing He (25 mL/min) for 1 h, each sample (100 mg) was cooled to 100 °C, and then adsorbed to saturation by NH_3 for 30 min. The physisorbed NH_3 was removed by flushing the sample with He (25 mL/min) for 1 h at the adsorption temperature. NH_3 desorption was carried out in the temperature range of 100–400 °C at ramp rate of 10 °C/min.

Fourier transform infrared (FT-IR) spectroscopy of pyridine adsorption measurements were performed on a Nicolet iS50 spectrometer equipped with a vacuum cell. Catalyst samples were pressed into self-supported disks (12–22 mg with diameter of 13 mm) and activated under vacuum (1×10^{-3} Pa) at 350 °C. After activation the samples were cooled to room temperature. A spectroscopy of the activated sample was recorded as background. Adsorption of pyridine was conducted at room temperature. Thermo gravimetric analysis (TG) was performed using a NET2SCH STA449F3 TGA analyzer with ramp rate of 10 °C/min from 25 to 800 °C in N_2 flow.

X-ray photoelectron spectroscopy (XPS) spectra were recorded with a Kratos AXIS Ultra ^{DLD}multi-technique X-ray photoelectron spectrometer, equipped with a monochromated Al Kα radiation (E = 1486.6 eV). The C 1 s peak with binding energy of 284.6 eV was taken as energy reference.

2.3. Catalytic tests

A two-necked round-bottom flask was used to carry out the liquid phase hydrogenation of FA. No pretreatment on the catalyst was conducted prior to reaction. The reactor was charged with FA (0.2 mL), solvent (4 mL) and catalyst (50 mg), and the mixture was stirred under ambient hydrogen pressure (balloon) at 25 °C for 1 h. The products were analyzed with flame ionization detector (FID) and capillary column DB-FFAP (30 m length and 0.25 mm internal diameter).

The spent catalyst was recovered by centrifugation washing with ethanol for three times, and then drying in vacuum. The activity of the recovered catalyst was tested under the same conditions as that applied for the fresh sample.

3. Results and discussion

3.1. Characterization of TNTs

Fig. 1 shows the XRD patterns of the commercial anatase-type TiO_2 and the TNTs. Diffraction peaks positioned at 9.8, 24 and 28° assigned to the titanates such as $Na_2Ti_2O_5{\cdot}H_2O$ and $Na_2Ti_3O_7$ are noticed on TNT (Fig. 1c) [18]. Upon calcination at 600 °C,

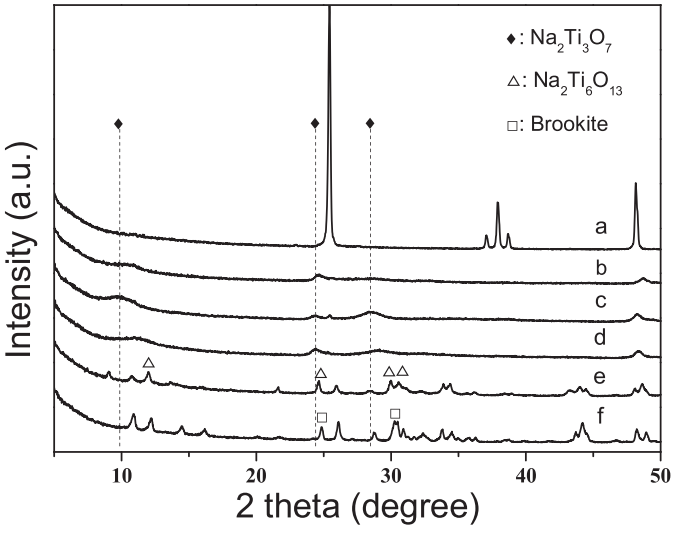

Fig. 1. XRD patterns of pristine anatase and different titanates (TNTs): (a) anatase; (b) TNT-H; (c) TNT; (d) TNT-400; (e) TNT-600; (f) TNT-800.

the titanates crystalline domains became enlarged according to the sharpening of the peaks, along with the appearance of weak peaks (12, 24.5, 29.8 and 30.5°) assigned to $Na_2Ti_6O_{13}$ for TNT-600 (Fig. 1e). After calcination at 800 °C, the intensity of $Na_2Ti_6O_{13}$ peaks slightly increased and new peaks assigned to brookite (24.6 and 30.6°) were found for TNT-800 (Fig. 1f), which could be derived from the dehydration of $Na_xTi_{2-x}Ti_2O_5{\cdot}H_2O$ and the removal of surface electrostatic charge [19]. After proton-exchange with 0.1 M HCl solution, there appears to be a decrease in the intensity of peak at 28° compared to that of 9.8 and 24° for TNT-H (Fig. 1b). This has been ascribed to the ionic exchange of Na^+ with H^+ in the titanates along with the phase transformation from $Na_2Ti_2O_5{\cdot}H_2O$ to $H_2Ti_2O_5{\cdot}H_2O$ [20].

SEM images of TNT and TNT-T (400, 600 and 800) are displayed in Fig. 2. The diameter and length of titanates with nanotube structure are in the range of 10–12 nm and 100–400 nm for TNT (Fig. 2a), respectively. It is believed that the sheet-like particles were rolling in to nanotubes during the washing [18]. After calcination at 400 °C, the morphology of TNT-400 (Fig. 2b) is almost identical to that of the TNT. Further increase of the temperature to 600 °C resulted in collapse of the nanotubes into rod-like structures with diameters of 50–70 nm (Fig. 2c), which is likely due to the dehydration of interlayered OH groups [21]. For TNT-800, the rod-like titanates agglomerated to cylindrical particles with length of 200–300 nm upon calcination at 800 °C (Fig. 2d).

Ammonia is a commonly used probe molecule to estimate the acidic amount and strength of the catalyst. From the results illustrated in Fig. 3, almost no desorption of NH_3 could be observed for anatase and TNT confirming that anatase and TNT do not possess strong acid sites. After proton-exchange with HCl, the amount of acid sites on TNT-H was 0.337 mmol g^{-1} and most ammonia desorbed in the range of 150–300 °C, indicating the presence of acid sites with moderate strength.

The acid property of the TNT and TNT-H was also investigated by pyridine adsorption FT-IR spectroscopy (Fig. 4). For both samples, the bands observed at ca. 1445 and ca. 1605 cm^{-1} are assigned to the adsorbed pyridine bound to Lewis acid sites (coordinative unsaturated Ti^{4+} sites) [22,23]. The slightly weak bands at ca. 1488 and ca. 1574 cm^{-1} are due to the ring breathing (υCCN, 19a and 8b) modes of pyridine molecules [23]. The two broad bands at 1540 and 1635 cm^{-1} were only observed on TNT-H. The appearance of these bands is resulted from the protonation of pyridine into pyridinium ions indicating the availability of Brønsted acid sites [22–24]. From this result, we can see that the proton-exchange of TNT leads to the generation of Brønsted acid sites on TNT-H which are absent on the surface of TNT.

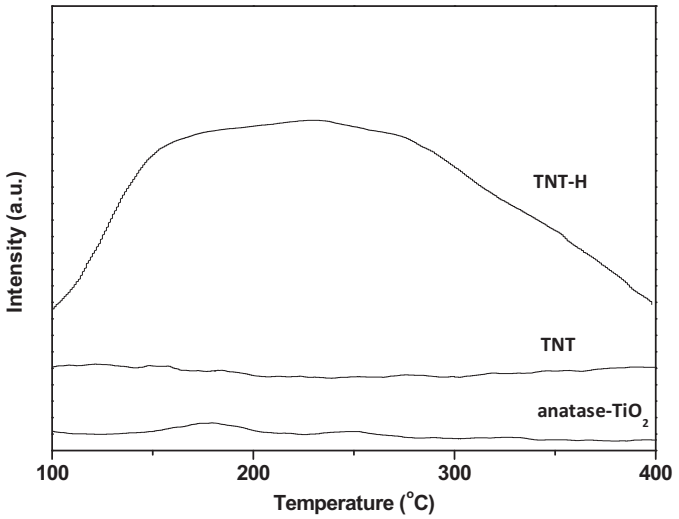

Fig. 3. NH_3-TPD profiles of pristine anatase and different titanates (TNT and TNT-H).

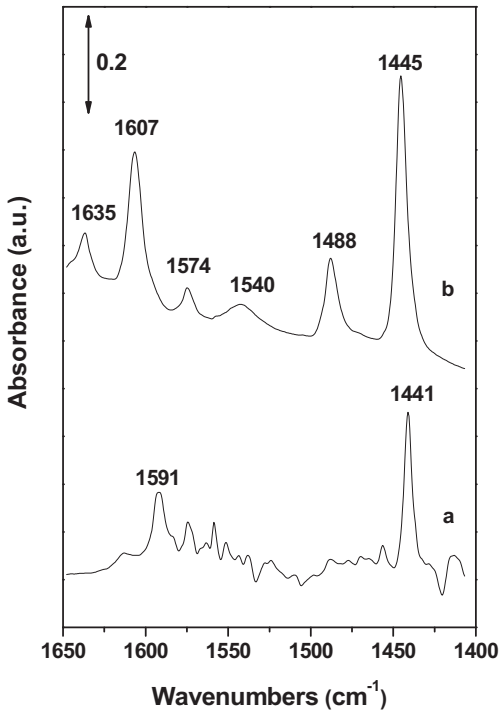

Fig. 4. Pyridine adsorption FT-IR spectra of TNTs: (a) TNT; (b) TNT-H after evacuation at room temperature.

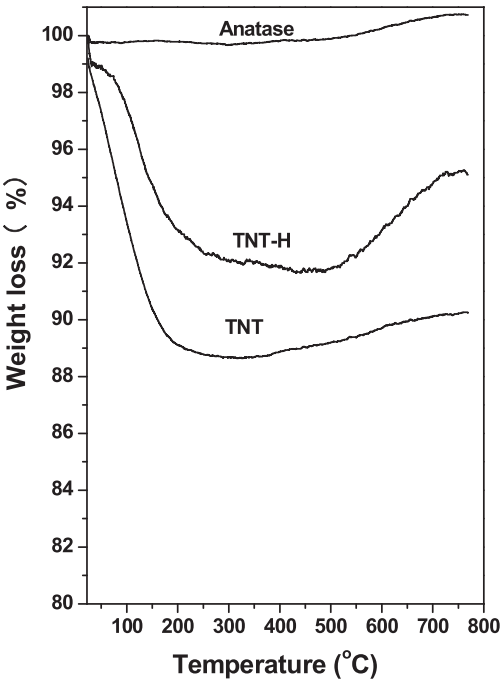

Fig. 5. The TG curves of pristine anatase and different titanates (TNTs) after adsorbing FA stream overnight.

The adsorption behavior of FA on these samples was studied by TG. TG curves for pristine anatase and different titanates (TNTs) after adsorbing FA vapor overnight are shown in Fig. 5. The TG curves of both TNT and TNT-H showed a broad peak (100–650 °C) centered at 350 °C relating to desorption of physisorbed FA. On the contrary, anatase did not show any remarkable weight loss

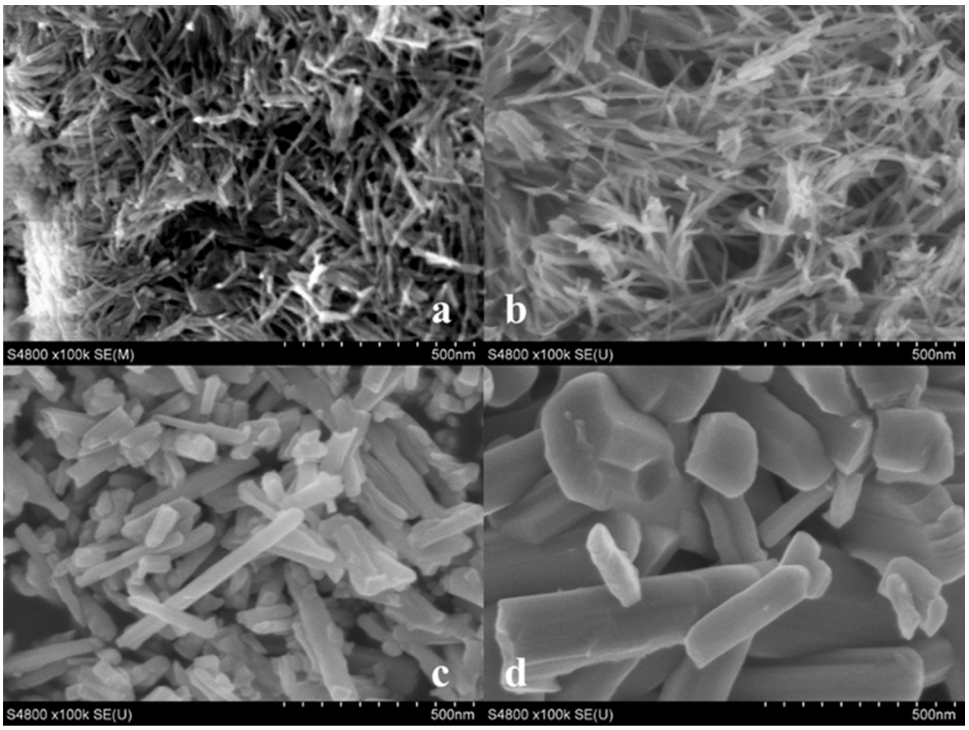

Fig. 2. SEM images of TNTs: (a) as prepared (TNT); (b) calcined at 400 °C (TNT-400); (c) calcined at 600 °C (TNT-600); (d) calcined at 800 °C (TNT-800).

Table 1
Structural properties of supports and supported Pd catalysts.

Catalysts	Pd loading[a] (wt.%)	SSA (m^2/g)	Dispersion[b] (%)
Anatase	–	8.3	–
TNT	–	31.4	–
5Pd/anatase	5.3	11.6	3.0
1Pd/TNT	1.3	107	27
3Pd/TNT	3.6	119	28
5Pd/TNT	5.8	95.1	26
10Pd/TNT	11.5	137	14
3Pd/TNT-H	3.3	126	10
5Pd/TNT-H	5.8	117	7.0
5Pd/TNT-400	7.1	77.4	27
5Pd/TNT-600	4.9	25.5	32
5Pd/TNT-800	5.2	11.2	13

[a] Determined by ICP-AES.
[b] According to pulse CO chemisorption.

indicating that FA hardly adsorbs on the anatase. This result suggests that both the acid sites (OH groups) and the surface O—Na species are responsible for the strong adsorption of FA on TNTs.

3.2. Characterization of Pd/TNTs

The BET specific surface areas (SSA) of the supports and Pd catalysts are shown in Table 1. The as-synthesized TNT sample showed surface area of 31.4 m^2/g, about 4 times higher than that of the pristine anatase material (8.3 m^2/g). After loading Pd, the resulting 5Pd/TNT had an even higher surface area of 95.1 m^2/g. This increase may arise from the structural evolution during the synthesis. It is believed that the surface area of TNT may substantially increase by treatment of acid washing due to the rolling of the $H_2Ti_3O_7$ sheets to tubes [25], which may also apply in this case because substantial amount of HCl was present in the Pd containing solution. This phenomenon may also be used to explain the large surface area of 3Pd/TNT-H and 5Pd/TNT-H (126 and 117 m^2/g, respectively). Upon calcination at 400, 600 and 800 °C, the surface area was 77.4, 22.5 and 11.2 m^2/g, respectively. The decrease of surface area is resulted by the collapse of tube structure during calcination.

The particle size and metal dispersion of palladium on TNTs were characterized by TEM and CO chemisorption, respectively. Typical TEM images of the supported Pd catalysts are shown in Fig. 6. Narrow distribution of palladium particle size (2–8 nm) was obtained for all catalysts and the average particle size is about 5.1 nm. The homogeneously distribution of palladium particles in small size (Fig. 6b and d) on TNT/TNT-H implies that palladium hydroxides were deposited on these supports uniformly during precipitation.

The CO chemisorption results are also listed in Table 1. The 5Pd/anatase catalyst used as a reference gave a dispersion of 3%. This very low Pd dispersion might be due to the extremely low surface area of anatase or a strong metal-support interaction (SMSI) between Pd and anatase surface [25–28]. For 1, 3 and 5Pd/TNT catalysts, Pd dispersion was close to 27%, which was substantially higher than that of 5Pd/anatase. The high Pd dispersion was probably attributed to the high surface area of TNT and the presence of residual sodium cation in the titanate. The latter point has been observed for TiO_2 support Pt and Pd catalysts by several research groups [29–31]. Higher Pd loading up to 10 wt.% led to a decrease of Pd dispersion to 14%. For Pd supported on TNT-H, the metal dispersion was relatively low and was close to 10%, which also points to the role of Na^+ in promoting Pd dispersion. For calcined TNTs, the Pd dispersion values of Pd/TNT-400, -600 and 800 were 27, 32 and 13%, respectively. We surmise that the poor textural properties of TNT-800 result in low dispersion of Pd.

To reveal the oxidation states of the supported Pd particles, the XPS core level spectra of Pd 3d of Pd/anatase, Pd/TNT, Pd/TNT-H were investigated and the deconvoluted XPS spectra are shown in Fig. 7. The Pd 3d peaks can be deconvoluted into two oxidation states, namely metallic Pd (~335 eV) and Pd^{2+} (~336.5 eV). The calculated abundance of two species is summarized in Table S1. For three catalysts the ratio of Pd^0 ranges from 45 to 65%. It can be found from Fig. 7 that the Pd $3d_{5/2}$ of Pd/anatase showed a significant lower BE of 334.6 eV, with respect to 335.3 eV of the 5Pd/TNT and

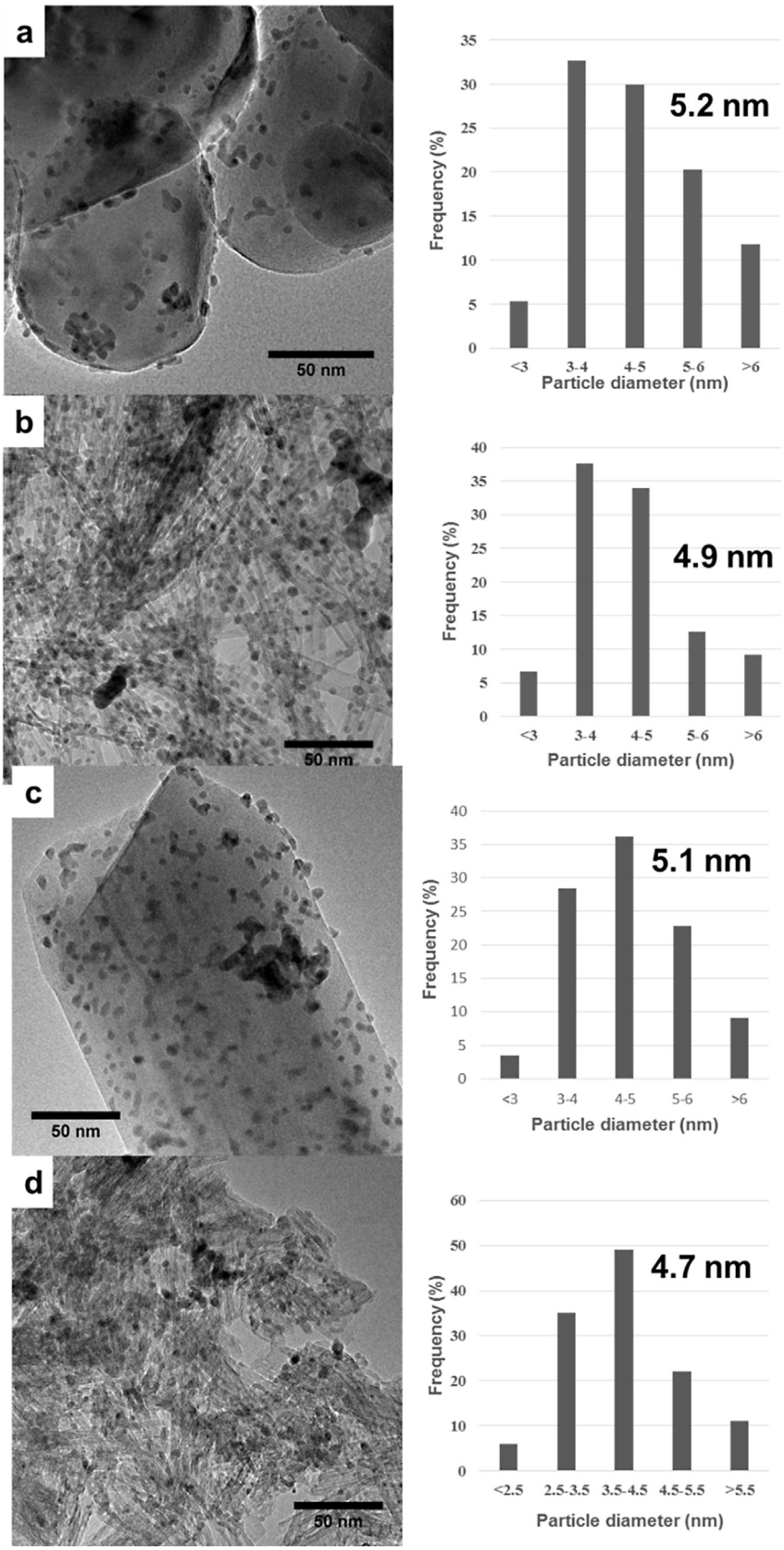

Fig. 6. TEM images (left) and particle size distributions (right) of supported Pd catalysts: (a) 5Pd/anatase; (b) 5Pd/TNT; (c) 5Pd/TNT-800; (d) 5Pd/TNT-H.

Table 2
Catalytic activity of supported Pd catalysts in furfuryl alcohol (FA) hydrogenation.[a]

Entry	Catalysts	Conv. (%)	Sel. (%)[b]		TOF
			THFA	MF	mol g^{-1} h^{-1}
1	5Pd/C[c]	68	65	32	0.62
2	5Pd/anatase	38	31	67	0.35
3	1Pd/TNT	6	100	0	0.21
4	3Pd/TNT	31	97	0	0.40
5	5Pd/TNT	75	96	1	0.60
6	10Pd/TNT	89	95	2	0.36
7	3Pd/TNT-H	14	75	20	0.20
8	5Pd/TNT-H	79	92	5	0.63
9	5Pd/TNT-400	66	92	6	0.43
10	5Pd/TNT-600	73	89	8	0.69
11	5Pd/TNT-800	12	64	32	0.11

[a] Reaction conditions: FA (0.2 mL), catalyst (50 mg), $C_2H_4Cl_2$ (4 mL), 25 °C, 1 h, H_2 balloon.
[b] Other side-product is the intermediates of partial-hydrogenation of one C=C bond in the furan ring.
[c] Commercial catalyst purchased from Alfa-Aesar.

335.5 eV of 5Pd/TNT-H. This result indicates that Pd nanoparticles are negatively charged on the $NaBH_4$ reduced Pd/anatase catalyst and the SMSI is present [32,33]. On the contrary, a relatively weak electronic interaction between Pd and TNT(-H) is noticed.

3.3. Catalytic activities of supported Pd catalysts

As an initial test, we first investigated the hydrogenation activities of supported Pd catalysts for FA in terms of conversion and selectivity by using $C_2H_4Cl_2$ as solvent (Table 2). $C_2H_4Cl_2$ is an interesting solvent which can render high hydrogenation or hydrogenolysis activity for supported Pd catalysts [34]. For Pd/TNT with loading of 1, 3, 5 and 10 wt.% (entries 3–6), the TOFs were 0.21, 0.40, 0.60 and 0.40 mol_{FA} g_{Pd}^{-1} h^{-1}, respectively. The highest TOF of THFA was obtained on 5Pd/TNT, which almost doubles the value of 5Pd/anatase (entry 2). The trend of turnover frequencies was in good agreement with that of the metal dispersion of Pd on TNTs. This result suggests that the unique porous tube-structure of titanate with high surface area favors the dispersion of Pd particles [35,36]. On the other hand, the stronger adsorption of FA on TNT than that on anatase may also lead to adsorption-enhanced hydrogenation/hydrogenolysis reactivity [37].

It should be noted that the selectivity of THFA exceeded 90% for Pd/TNT catalysts (entries 3–6), while it was only 31% on 5Pd/anatase catalyst (entry 2). The dominant product in FA hydrogenation on 5Pd/anatase is MF. It has been proposed that MF is produced via a hydrogenolysis reaction pathway which takes place on the oxidized Pd^{2+} according to a recent study [34]. The presence of both Pd^{2+} and Pd^0 species are undoubtedly confirmed by XPS (Fig. 7) in our case. Therefore we speculate that the metallic Pd catalyzes the hydrogenation reaction, which competes with the hydrogenolysis on Pd^{2+} in this process. Both reaction pathways were also clearly observed on a commercial 5Pd/C catalyst (entry 1), which showed 68% FA conversion and 32% selectivity to MF. This finding is consistent with previous reports [38–43]. Bradley et al. [38] have shown that Pd can readily adsorb furan ring due to a strong interaction between the metal and the π bonds in the molecule. The strong interaction, due to a re-hybridization of the carbon bonds from sp^2-to-sp^3 has been proposed to occur on Pd, which may account for the formation of THFA. Pang and Medlin [39] have found that furfuryl alcohol underwent C—O scission yielding MF as a product. The DFT calculation results suggested that the adsorption of C—O bond of hydroxyalkyl species paralleling to the Pd (1 1 1) surface may also favor the C—O scission therefore yielding MF [39–42]. Interestingly, this reaction pathway can be inhibited by potassium promoter [39,43], which well

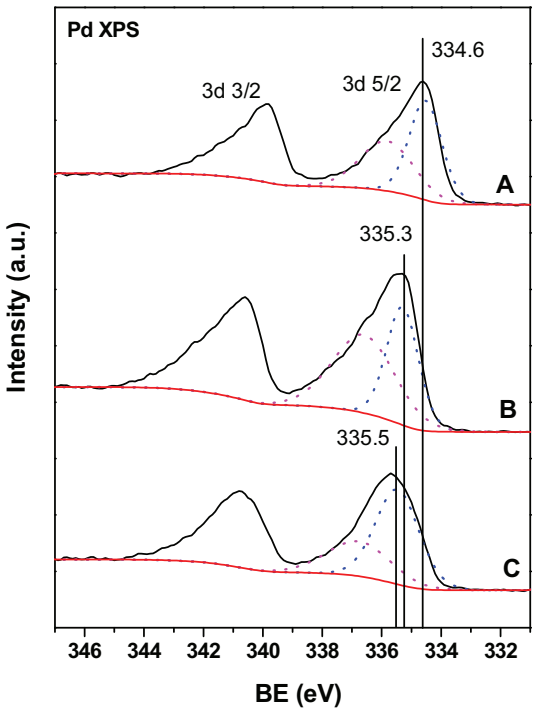

Fig. 7. Pd 3d XPS spectra of supported Pd catalysts: (A) 5Pd/anatase; (B) 5Pd/TNT; (C) 5Pd/TNT-H.

explains the very low yield of MF in Pd/TNTs. Indeed, when Na^+ was exchanged by proton, higher MF selectivity was noticed as observed for 3Pd/TNT-H catalyst (entry 7). However, this reaction pathway change is not pronounced for 5Pd/TNT-H (entry 8), probably because of the very high hydrogenation activity for high Pd loading catalysts. Also shown in Table 2 is the effect of calcination temperature of TNT on the catalytic activity of supported Pd catalysts. The TOFs of Pd/TNT-400, 600, and 800 are 0.43, 0.69, and 0.11 mol_{FA} g_{Pd}^{-1} h^{-1}, respectively. Pd/TNT-600 showed the highest TOF and THFA selectivity of 89% (entry 10). In contrast, Pd/TNT-800 (entry 11) showed the lowest activity (12% FA conversion) as well as the highest selectivity to MF (32%) among three catalysts. This result points to the effect of surface changes upon calcination on the catalytic activity. The SEM images (Fig. 2d) showed that the morphology of TNT-800 was cylindrical particles with diameter varying from 0.2 to 1 μm. These large particles had very low SSA (11 m^2/g). Moreover, the surface structure probably relates to the brookite crystalline. We therefore speculate that the distinct different catalytic behavior of Pd/TNT-800 relates to these structural changes.

3.4. Solvent effect, kinetics and reusability

The reaction performed in $C_2H_4Cl_2$ proceeded smoothly, yet cleaner solvents are desirable. Therefore the hydrogenation in other solvents (ethanol, isopropanol, toluene, heptane and water) was conducted and the results are shown in Table 3. The reactivity follows the trend of ethanol > $C_2H_4Cl_2$ > isopropanol > toluene > heptane > H_2O. Ethanol gave the best catalytic performance amongst the solvents investigated, and the selectivity to THFA was the highest (98%) with minute production of MF. This result emphasizes the essential role of solvent used in determining the hydrogenation activity [44]. Compared with water, alcohols have a better H_2 solubility and can also stabilize the reactive intermediates [45,46]. When heptane and toluene were used, the catalyst particles were not

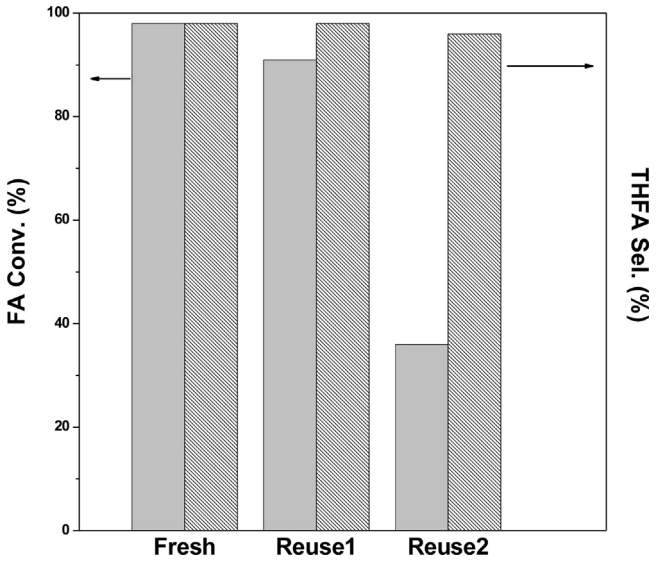

Fig. 8. Recycle study of 5Pd/TNT for FA hydrogenation. Reaction conditions: FA (0.2 mL), 5Pd/TNT (50 mg), ethanol (4 mL), 25 °C, 1 h, H_2 balloon.

well dispersed and probably led to diffusion-limitations even upon very high stirring rate. The results suggested that alcohols are suitable solvents for this reaction.

We also investigated the effects of initial FA concentration, and hydrogen pressure on the catalytic performances (Tables S2 and S3). The results suggested that that the THFA selectivity did not change with the increase in initial FA concentration. Meanwhile the TOF was slightly increased with the increase in FA concentration. This phenomenon may be explained by the competitive adsorption of product (THFA) and reactants (hydrogen and FA) on the catalyst surface [1]. It was also observed that the TOF increased with the increase of hydrogen pressure (Table S3) and the reaction order with respect to hydrogen was estimated to be 0.2. Increasing the reaction temperature from 25 to 50 °C led to slightly decrease of FA conversion by 20%. This result probably implies that the adsorption of reactants (probably FA) is inhibited at high temperature. Further increase of temperature is not desirable since the FA easily undergoes polymerization.

The recyclability of 5Pd/TNT catalyst was evaluated through three repeated reactions in ethanol and the results are shown in Fig. 8. It shows that the catalytic performance of the 5Pd/TNT catalyst remains almost the same after the first time, but the activity of the catalyst dropped drastically after being used two times. Chemical analysis (ICP) of the catalyst after reaction revealed no leaching of Pd. The activity loss after two runs of reaction may be due to the strong adsorption of FA or possible polymerization of FA on the catalyst [42,47]. To our delight the selectivity to THFA of the Pd/TNT was maintained. Further study is necessary to achieve high reusability of this catalyst by structural modification.

Table 3
Catalytic performance of 5Pd/TNT for FA hydrogenation in various solvents.[a]

Solvent	Conv. (%)	Sel. (%)[b]	
		THFA	MF
H_2O	29	99	0
Heptane	43	97	3
Toluene	48	98	1
Isopropanol	70	99	0.4
$C_2H_4Cl_2$	75	96	1
Ethanol	98	98	0.4

[a] Reaction conditions: FA (0.2 mL), 5Pd/TNT (50 mg), solvent (4 mL), 25 °C, 1 h, H_2 balloon.
[b] Other side-product is the intermediate of partial-hydrogenation of one C=C bond in the furan ring.

4. Conclusion

In summary, TNT with $Na_2Ti_2O_5{\cdot}H_2O$ and $Na_2Ti_3O_7$ structures was prepared by a hydrothermal method and used as support of Pd nanoparticles. This Pd/TNT was found to be highly active in FA hydrogenation under mild conditions (25 °C, H_2 balloon). 5Pd/TNT showed the highest turnover frequency of 0.60 $mol_{FA}\ g_{Pd}^{-1}\ h^{-1}$. The effect of different solvents on the catalysis was also conducted and the ethanol gave the best catalytic performance (98% conversion of FA and 98% selectivity to THFA) amongst the solvents investigated. The performance of the catalyst is strongly affected by the nature of Pd and the unique surface structure of TNT showing strong FA adsorption ability.

Acknowledgement

We acknowledge the financial support from the National Natural Science Foundation of China (Grant No. 21203065).

Appendix A. Supplementary data

Supplementary data associated with this article can be found, in the online version, at http://dx.doi.org/10.1016/j.apcata.2015.09.034.

References

[1] M.A. Tike, V.V. Mahajani, Ind. Eng. Chem. Res. 46 (2007) 3275–3282.
[2] K. Othmer, Encyclopedia of Chemical Technology, Vol. 12, 5th ed., Wiley Interscience Publication, New York, 2004.
[3] S. Koso, I. Furikado, A. Shimao, T. Miyazawa, K. Kunimori, K. Tomishige, Chem. Commun. 15 (2009) 2035–2037.
[4] S. Koso, N. Ueda, Y. Shinmi, K. Okumura, T. Kizuka, K. Tomishige, J. Catal. 267 (2009) 89–92.
[5] J.G. Stevens, R.A. Bourne, M.V. Twigg, M. Poliakoff, Angew. Chem. Int. Ed. 49 (2010) 8856–8859.
[6] K. Yan, G.S. Wu, T. Lafleur, C. Jarvis, Renew. Sust. Energy Rev. 38 (2014) 663–676.
[7] A.S. Gowda, S. Parkin, F.T. Ladipo, Appl. Organomet. Chem. 26 (2012) 86–93.
[8] H. Adkins, R. Connor, J. Am. Chem. Soc. 53 (1931) 1091–1095.
[9] R.M. Lukes, L.S. Nelson, J. Org. Chem. 21 (1956) 1096–1098.
[10] X.C. Chen, W. Sun, N. Xiao, Y.J. Yan, S.W. Liu, Chem. Eng. J. 126 (2007) 5–11.
[11] M. Hronec, K. Fulajtarova, T. Sotak, Appl. Catal. B: Environ. 154 (2014) 294–300.
[12] Y. Nakagawa, H. Nakazawa, H. Watanabe, K. Tomishige, ChemCatChem 4 (2012) 1791–1797.
[13] N. Merat, C. Godawa, A. Gaset, J. Chem. Tech. Biotechnol. 48 (1990) 145–159.
[14] B. Zhang, Y. Zhu, G. Ding, H. Zheng, Y. Li, Green Chem. 14 (2012) 3402–3409.
[15] N.S. Biradar, A.A. Hengne, S.N. Birajdar, R. Swami, C.V. Rode, Org. Process Res. Dev. 18 (2014) 1434–1442.
[16] D.J. Cole-Hamilton, Science 299 (2003) 1702–1706.
[17] F. Khan, A. Vallat, G. Süss-Fink, Catal. Commun. 12 (2011) 1428–1431.
[18] Q. Chen, W.Z. Zhou, G.H. Du, L.M. Peng, Adv. Mater. 14 (2002) 1208–1211.
[19] J.N. Nian, H. Teng, J. Phys. Chem. B 110 (2006) 4193–4198.
[20] J. Yang, Z. Jin, X. Wang, W. Li, J. Zhang, S. Zhang, X. Guo, Z. Zhang, Dalton. Trans. 20 (2003) 3898–3901.
[21] L. Zhang, H. Lin, N. Wang, C. Lin, J. Li, J. Alloys Compd. 431 (2007) 230–235.
[22] M. Kitano, E. Wada, K. Nakajima, S. Hayashi, S. Miyazaki, H. Kobayashi, M. Hara, Chem. Mater. 25 (2013) 385–393.
[23] M.I. Zaki, M.A. Hasan, F.A. Al-Sagheer, L. Pasupulety, Colloids Surf. A: Physicochem. Eng. Aspects 190 (2001) 261–274.
[24] S. Li, N. Li, G. Li, L. Li, A. Wang, Y. Cong, X. Wang, G. Xu, T. Zhang, Appl. Catal. B: Environ. 170–171 (2015) 124–134.
[25] T. Kasuga, M. Hiramatsu, A. Hoson, T. Sekino, K. Niihara, Adv. Mater. 11 (1999) 1307–1311.
[26] N.S. Babu, N. Lingaiah, N. Pasha, J.V. Kumar, P.S.S. Prasad, Catal. Today 141 (2009) 120–124.
[27] P. Weerachawanasak, O. Mekasuwandumrong, M. Arai, S. Fujita, P. Praserthdam, J. Panpranot, J. Catal. 262 (2009) 199–205.
[28] J.H. Kang, E.W. Shin, W.J. Kim, J.D. Park, S.H. Moon, J. Catal. 208 (2002) 310–320.
[29] L. Nie, J. Yu, X. Li, B. Cheng, G. Liu, M. Jaroniec, Environ. Sci. Technol. 47 (2013) 2777–2783.

[30] C. Zhang, Y. Li, Y. Wang, H. He, Environ. Sci. Technol. 48 (2014) 5816–5822.
[31] A.N.A.J. Ardila Reyes, E. Arriola, J.A. Hernández, G.A. Fuentes, Appl. Catal. A: Gen. 497 (2015) 211–215.
[32] H. Huang, D.Y.C. Leung, ACS Catal. 1 (2011) 348–354.
[33] O. Mekasuwandumrong, S. Phothakwanpracha, B. Jongsomjit, A. Shotipruk, J. Panpranot, Catal. Lett. 136 (2010) 164–170.
[34] S. Iqbal, X. Liu, O.F. Aldosari, P.J. Miedziak, J.K. Edwards, G.L. Brett, A. Akram, G.M. King, T.E. Davies, D.J. Morgan, D.K. Knight, G.J. Hutchings, Catal. Sci. Technol. 4 (2014) 2280–2286.
[35] W.J. Shen, M. Okumura, Y. Matsumura, M. Haruta, Appl. Catal. A: Gen. 213 (2001) 225–232.
[36] X. Yang, L. Wu, L. Ma, X. Li, T. Wang, S. Liao, Catal. Commun. 59 (2015) 184–188.
[37] J. Shi, R. Nie, P. Chen, Z. Hou, Catal. Commun. 41 (2013) 101–105.
[38] M.K. Bradley, J. Robinson, D.P. Woodruff, Surf. Sci. 604 (2010) 920–925.
[39] S.H. Pang, J.W. Medlin, ACS Catal. 1 (2011) 1272–1283.
[40] S. Sitthisa, T. Sooknoi, Y. Ma, P.B. Balbuena, D.E. Resasco, J. Catal. 277 (2011) 1–13.
[41] S. Sitthisa, D.E. Resasco, Catal. Lett. 141 (2011) 784–791.
[42] M. Hronec, K. Fulajtarova, T. Liptaj, Appl. Catal. A: Gen. 437 (2012) 104–111.
[43] W. Zhang, Y. Zhu, S. Niu, Y. Li, J. Mol. Catal. A: Chem. 335 (2011) 71–81.
[44] J. Lang, E. van der Heide, J. van Buijtenen, R. Price, ChemSusChem 5 (2012) 150–166.
[45] X. Hu, R.J.M. Westerhof, D. Dong, L. Wu, C.Z. Li, ACS Sustain. Chem. Eng. 2 (2014) 2562–2575.
[46] X. Xu, C. Lievens, C.Z. Li, ChemSusChem 5 (2012) 1427–1434.
[47] M. Hronec, K. Fulajtarova, M. Micusik, Appl. Catal. A: Gen. 468 (2013) 426–431.